# A DISPERSED GENERATION SYSTEM BASED ON PHOTOVOLTAIC CELLS: CONVERTER CONFIGURATION AND SWITCHING STRATEGY

*Ricardo L. Carletti, Luís Cláudio G. Lopes and Pedro G. Barbosa*

Federal University of Juiz de Fora
Department of Electrical Engineering
P.O. Box 422
36.001-970 - Juiz de Fora – MG

carletti@eletrica.ufjf.br, gamboa@eletrica.ufjf.br
and pedro.gomes@ufjf.edu.br

***Abstract*** **- This paper presents the basic principles of operation of Dispersed Generation System (DGS) based on photovoltaic cells, which will be implemented at Federal University of Juiz de Fora (UFJF). The DC-AC converter configuration is discussed as well as the switching strategy applied to improve the output voltage waveform with the minimum number of static power converters. Some characteristics of the converter will be investigated and discussed using simulation results obtained with the ATP/EMTP (Electromagnetic Transients Program) simulation package.**

*Keywords – Dispersed Generation System, multipulse converter, programmed harmonic elimination-PWM.*

## I. INTRODUCTION

In 1992 fifty-eight hydroelectric power plants were under construction or being studied for future projects in Brazil [1]. However, ten years later, the Brazilian community had a rationing program of electric energy as a consequence of the outflow of investments in this area and due to the reduction of the hydraulic energy storage at the dams, which is strongly dependent on the climate conditions.

Considering this peculiar scenario in Brazil and the increase of the power demand in most of the consumer centers, electric utility companies, research centers and universities are very much interested in the studies involving new solutions to improve the offering of electric energy. Thus, microturbines, fuel cells, photovoltaic systems, wind energy systems, batteries storage energy systems, gas turbines among other technologies, in the range from few *kW* to hundreds *kW*, are possible alternative technologies for dispersed electrical energy generation systems applications and are expected to become more economically feasible [2].

However, the connection of these alternative energy sources into the utility AC system must be done through static power converters (SPC) which primary function is to perform the energy conversion from the alternative source to AC utility system. Fig. 1 shows a schematic diagram of a Dispersed Generation System (DGS) based on photovoltaic (PV) cells to be analyzed in this work. The DC-DC converters drain the energy from the photovoltaic arrays and feed the DC link, which is coupled to the AC network by DC-AC static power converter.

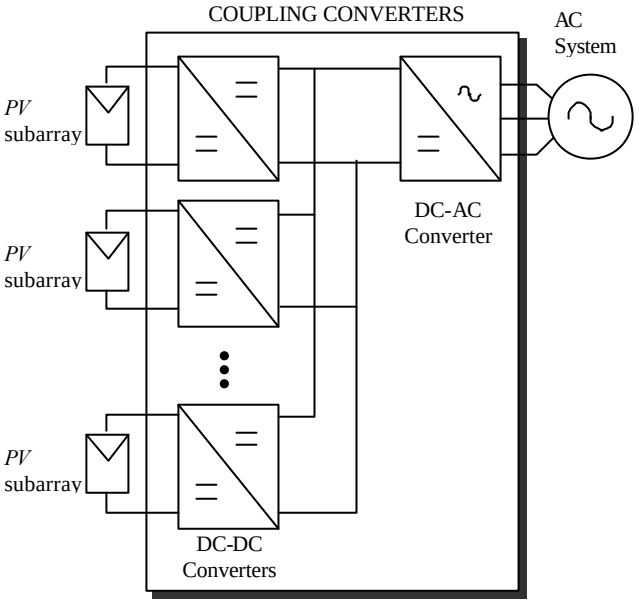


Fig. 1: Functional block diagram of a DGS based on PV cells.

In spite of being a very attractive alternative, the feeding of energy generated by a PV cell into an existing AC grid poses some problems to the control of the DC-AC converters that connect the two systems. Although static power converters generate voltages and currents with variable amplitude and frequency, they have the disadvantage of generating harmonic components in its AC terminals that can cause distortions in the power system.

There is a practical agreement in medium and high power photovoltaic generation plant to group the photovoltaic cells in sub arrays with output power not

higher than 3 *kW*. This criterion was adopted to reduce the DC-DC converters cable losses, to simplify the galvanic protection of the PV cells and to permit the safety operational maintenance by the technical staff in the case of switch off a sub array. However in the case of the coupled static power converter, the DC-AC converter topology will depend on the DC link characteristic. In this way the SPC can be a VSC (Voltage Source Converter) or a CSC (Current Source Converter) if the DC link is viewed as a constant voltage source or current source, respectively.

The objective of this work is to present the modeling and the analysis of operation of a DC-AC voltage source converter of a 30 *kW* dispersed generation plant based on photovoltaic cells at the Campus of Federal University of Juiz de Fora (UFJF). The static power converter was modeled as a three-phase VSC with a DC link capacitor. This system should transfer the energy from the DC link to the three-phase AC system with minimum harmonic distortion and with controlled active and reactive powers at the converter terminals. The Alternative Transients Program / Electromagnetic Transients Program (ATP / EMTP) was used to model, to simulate and to test the performance and feasibility of the converter configuration and its control strategy.

## II. Converter Configuration and Switching Strategies

The development of high capacity self-commutated semiconductor switches such as GTOs (*Gate Turn-off Thyristors*), GCTs (*Gate Commutated Thyristors*) and IGBTs (*Insulated Gate Bipolar Transistors*) has made the design of VSCs (Voltage Source Converters) easier. Fig. 2 shows the basic topology of a three-phase VSC based on six IGBTs with six anti-parallel diodes. These converters have been widely used in industrial applications and most recently in the area of high power transmission and distribution systems (FACTS –*Flexible AC Transmission Systems* and *Custom Power*) [3] and [4].

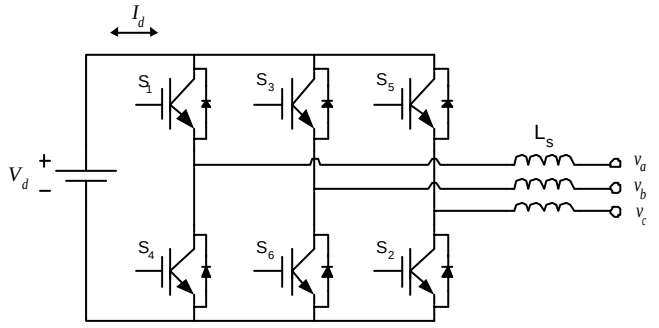


Fig. 2: Three-phase Voltage Source Converter.

It is generally considered that Pulse Width Modulation (PWM) switching strategy of medium and high power VSC should be as high as possible [5]. This is probably a consequence of the performance of industrial converters such as adjustable speed drives (ASD), active power filters (APF), uninterruptible power supplies (UPS), etc. However the main disadvantage of the usage of high-frequency PWM-VSC in high-power applications is that the switching losses become critical. In these applications, the square wave operation will promote maximal utilization of the output voltage, low stress on the switches and reduce switching losses.

Despite the better utilization of the semiconductor switches obtained with the reducing of the switching frequency, low order harmonics are generated at the VSCs terminals. Thus, multipulse VSCs could be used, as harmonic neutralization method, to remove lower harmonics components of the square wave voltage waveform. Multipulse VSCs combine two or more square wave converter output voltages, operating with suitable phase differences, through a magnetic structure (phase-shifting transformers) in such a way that the harmonics generated by one converter is cancelled by other and so on.

Many works suggested several possible usages of multipulse VSCs, with 100 *MVA* or higher [6]-[7], operating as shunt and series reactive power compensator to synthesize synchronous AC voltage to be connected in parallel and in series with an AC transmission line. In these applications the number of VSC connected in series is more than four (24 pulse or higher VSCs).

Fig. 3 shows a basic topology of a multistage converter based on the connection of two VSC through two Y-Y e -Y. Fig. 4 (a) and (b) show the output voltage waveform and its harmonic spectrum considering a DC voltage without ripple. In this converter configuration, assuming that each converter is switched at the fundamental frequency (60 *Hz*), the fifth and seventh harmonics are cancelled, as well as all those with order of 5 or 7 plus multiples of 12.

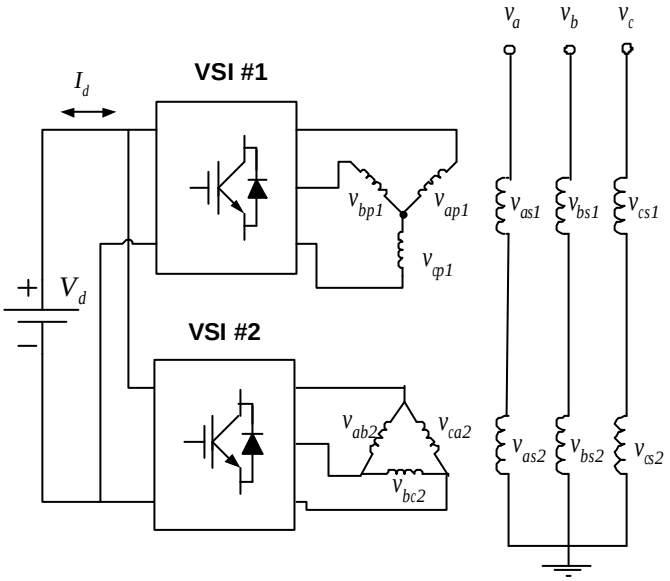


Fig. 3: Configuration of 12-pulse VSC.

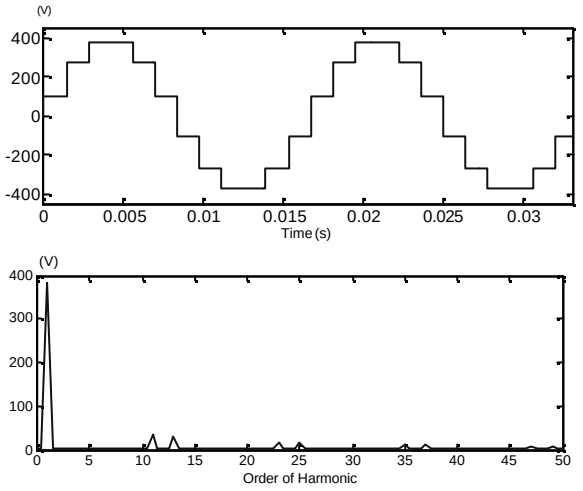


Fig. 4: (a) Voltage waveform of 12-pulse VSC; (b) harmonic spectrum.

On the other hand, in the case of medium to high power applications such as dispersed and storage generations system (DGS), an attractive approach to reduce the initial cost of the installation can be achieved by using a hybrid configuration for the converters that combine a low number of VSC and a low switching frequency PWM technique.

Thus, to remove some harmonics components not neutralized in the 12-pulse connection a programmed PWM was implemented in the previous converter configuration as will be shown in the next section.

## III. PROGRAMMED HARMONIC ELIMINATION TECHNIQUE

Using suitable switching angles [8] in each phase of the VSC of Fig. 3, the lower order harmonics showed in Fig. 4(b) could be suppressed without the use of high-frequency carrier PWM [9]. Fig. 5 shows an example of the phase "*a*" output voltage of a three-phase converter with a generic *M* number of notches per half-cycle.

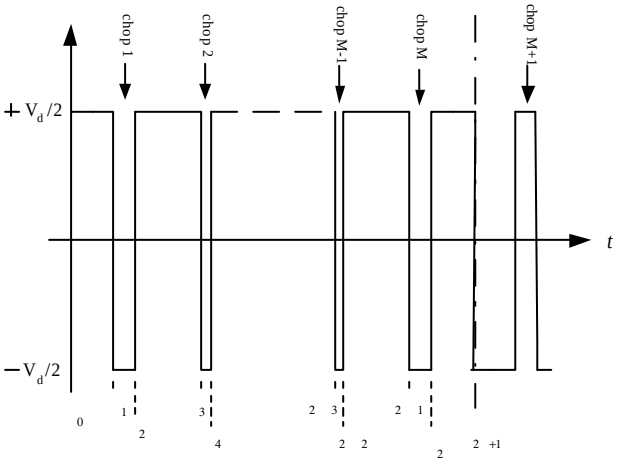


Fig. 5: Generic output phase voltage of a three-phase VSI with *M* notches per half-cycle.

If the voltage waveform showed in Fig. 5 is expanded on a Fourier series, the mathematical expression of the *nth* harmonic in the output voltage is given by:

$$V_n = \frac{2}{n} V_d \left[1 + 2\sum_{k=1}^{M} (-1)^k \cos(n\alpha_k)\right], \quad (1)$$

where, $n$ is the order of the voltage harmonic; $M$ is the number of notches per half-cycle of the fundamental frequency, $\alpha_k$ are the angles of the programmed PWM notches in (*rad*) and $k$ =1, 2, 3...

Based on (1) if the voltage waveform shown in Fig. 5 has two notches per half-cycle the converter switching frequency will be 5 times higher than the output voltage fundamental frequency, that is, 5 x 60 $Hz$ = 300 $Hz$. Therefore, looking back to the harmonic spectrum shown in Fig. 4 (b), it is possible to remove the 11th and 13th harmonics in the 12-pulse VSC output voltages. Thus, rewriting (1) for $M$ = 2 yields:

$$V_n = \frac{2}{n} V_d \left[1 - 2\cos(n\alpha_1) + 2\cos(n\alpha_2)\right] \quad (2)$$

Then, the angles $\alpha_1$ and $\alpha_2$ that will carry out the above task could be calculated solving (2) for $V_{11}$ = 0 and $V_{13}$ = 0, respectively. Since the system is a non-linear system and the notches do not control the fundamental component of the output voltage, there are several sets of angles that satisfy (2) and the best result can be obtained for $\alpha_1$ and $\alpha_2$ equals to 36.43º and 39.55º, respectively. Fig. 6 (a) and (b) show the phase voltage waveform and its harmonic spectrum, respectively. Note that the magnitude of the harmonics, with order higher than the eliminated harmonics, increases. However, the 23rd harmonic component, presented in the output voltage of the 12-pulse VSC, was also removed. This behavior is due to the necessary angles to cancel the 11th and the 23rd harmonics that are too close to those calculated to eliminated the 11th and the 13th harmonics, *i.e.*, $\alpha_1$=36.47º and $\alpha_2$=39.58º, respectively.

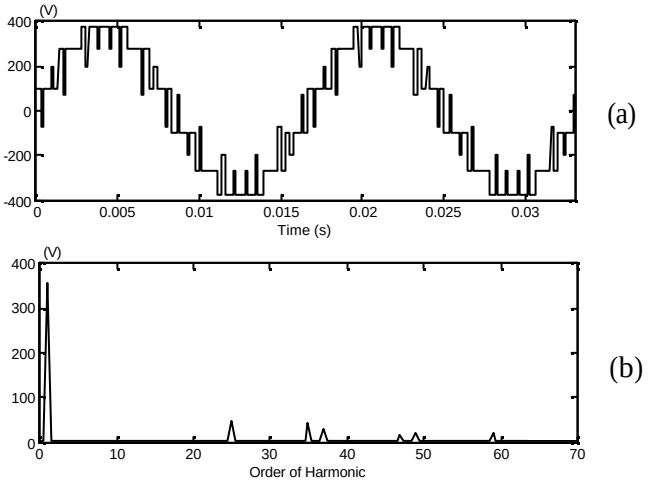


Fig. 6: (a) 12-pulse VSC voltage waveform for 2 notches per half-cycle; (b) harmonic spectrum.

In this way, if an additional notch is included in each VSC output voltage the 11th, the 13th and the 23rd harmonics can be removed. In this case the VSCs are switched with a frequency 7 times higher than the fundamental frequency (7 x 60 $Hz$ = 420 $Hz$). Using the same methodology applied before, for $M = 4$, the switching angles $_1$, $_2$ and $_3$ are 4.14º, 11.34º and 13.09º, respectively. Fig. 7 (a) shows the output VSC voltage waveform and Fig. 7 (b) shows its harmonic spectrum. As explained previously the set of angles obtained solving (2) for $_1$, $_2$ and $_3$ is too close to the solution that also eliminates (*minimizes*) the 25th harmonic.

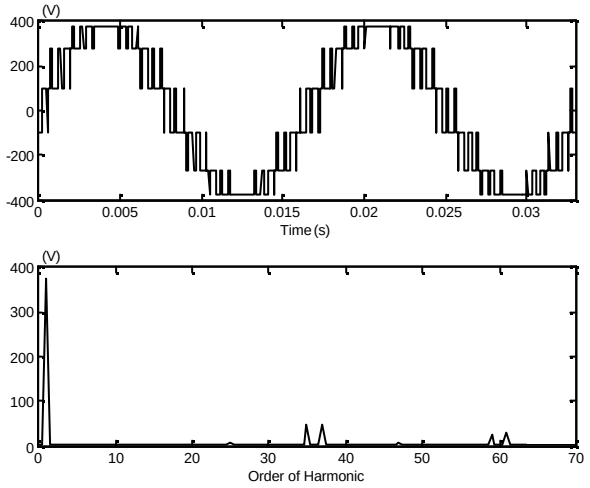


Fig. 7: (a) 12-pulse VSC voltage waveform with harmonic neutralization with 3 notches per half-cycle; (b) harmonic spectrum.

From Fig. 7 (b), it is possible to conclude that this converter configuration works as 36-pulse VSC (6 converters connected in series). Since this voltage waveform does not contain low order harmonics, a small LC filter can be designed using the leakage inductance of the connection transformers. In the next section, some digital simulation results obtained with the VSC modeled in the ATP/EMTP package will be shown.

## IV. DIGITAL SIMULATION RESULTS

The 12-pulse VSC with programmed harmonic elimination switching (VSC-12pHE) was modeled using ATP/EMTP simulation package [10]. Since the notches did not control the fundamental component of voltage waveform of the VSC, a phase control was used to assure that the energy drained from the PV array goes to the AC system. The photovoltaic cells and the DC-DC converter was modeled by a controllable current source connected in parallel with a 1500 $F$ DC link capacitor as shown in Fig. 8. The turn-ratios of the transformers and the magnitude of system voltages are indicated in this figure.

The multipulse with programmed harmonic elimination converter is controlled to generate three-phase output voltages with the same magnitude and phase of AC system voltages. When the DC-DC converter, shown in Fig. 1, charges the DC capacitor with the electrical energy drained from the PV cells, the set of three-phase VSC-12pHE output voltages will increase their magnitude. This action will force a non-null value of instantaneous reactive power at the VSC terminals. Then, the controller changes the VSC output voltages phase angle in such a way to force an active power flow into the AC system, discharging the DC capacitor.

Fig. 9 shows the control block diagram of the VSC-12pHE. The control algorithm uses the concept of instantaneous real and imaginary power theory and it is similar to the control proposed for a STATCOM [11]. However, as explained before, the main objective here is not to drain or to inject some amount of instantaneous imaginary power but it is injected the instantaneous real power, from the photovoltaic cells, into the AC power system.

The phase angle of the source voltage ( ) is obtained from a digital PLL (*Phase Locked-Loop*) implemented as shown within dashed line. The instantaneous three phase system voltages and currents are used to calculate the instantaneous imaginary power $q$ at the converter

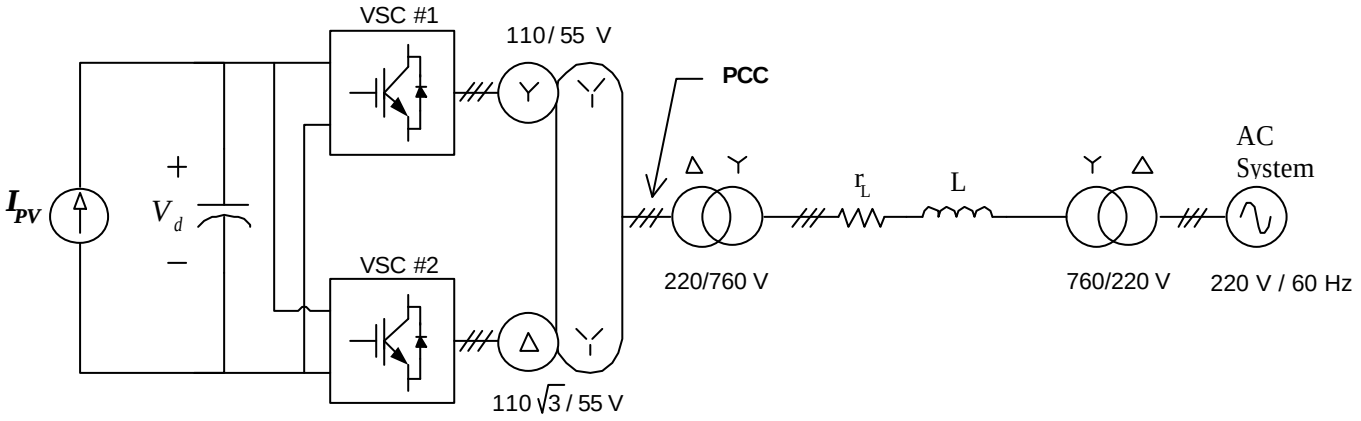


Fig. 8: Single line diagram of the modeled photovoltaic generation plant in the ATP/EMTP.

terminals. The error between the desired and measured imaginary instantaneous powers feeds a proportional-integral controller, which output is the reference phase angle ( *) of the converter output voltages. Then, the phase angle * is added to the detected AC system frequency and phase signal = ( t+ ). The composed signal is sent to the Phase Comparator Block to generate the turn-on and turn-off signals of the semiconductor switches. However to neutralized some of the voltages harmonics, the angles 1, 2 and 3, determined in the previous section, are pre-programmed into the Phase Comparator Block.

Fig. 10 shows the control signals generated by the PLL added to the output of the imaginary power controller and the normalized system voltage. Note that the control signal ( + *) used to feed the phase comparator of the VSC#2 is phase-shifted by - /6 *rad* (-30º) in relation to the signal to of the VSC#1. This extra delay is necessary since the -Y transformer leads /6 *rad* the output voltages of VSC#2 with respect to the output voltages of the VSC#1.

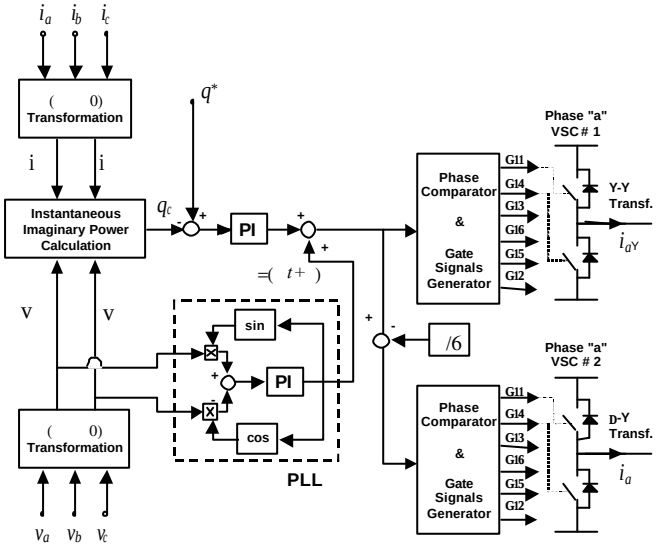


Fig. 9: Control block diagram of the VSC 12p-HE.

In order to confirm the efficiency of the switching and control strategies, computer simulation results are presented. Initially, the VCS12pHE is in stand-by, that is, there is no real or imaginary powers flowing to the AC system. Then, in $t$ = 0.05 s, the photovoltaic cells injects 25 *kW* of real power into the DC link of the VSC-12pHE. The DC link capacitor voltage increases and consequently the magnitude of the output voltages of the VSC-12pHE. Since the converter output voltages are changed, the instantaneous imaginary power at the VSC terminal also varies and the proportional-integral controller shown in Fig. 9 is fed by a non-null input error. The PI controller changes the reference phase angle ( *) of the converter output voltages in such a way to force the real power that is coming from the photovoltaic cells to flow to the AC system, discharging the DC link capacitor. Finally, at $t$ = 0.3s, the imaginary power reference signal $q^*$ is step changed from 0 to –15 *kvai* to show the ability of the proposed installation to compensate reactive power at the converter terminals.

Fig. 11 shows the converter phase *'a'* output voltage. Fig. 12 shows the VSC12pHE voltage output and the line current at PCC (*Point of Common Coupling*). Fig. 13 and Fig. 14 show the instantaneous real and imaginary powers at the VSC output terminals, respectively. Fig. 15 shows how the VSC 12p-HE DC link voltage varies during the transients. Fig. 16 shows a detail of the VSC12pHE voltage output and line current.

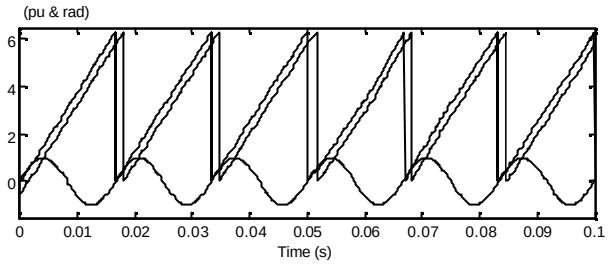


Fig. 10: Control signals of VSC#1 and VSC#2 and phase "*a*" normalized AC system voltage.

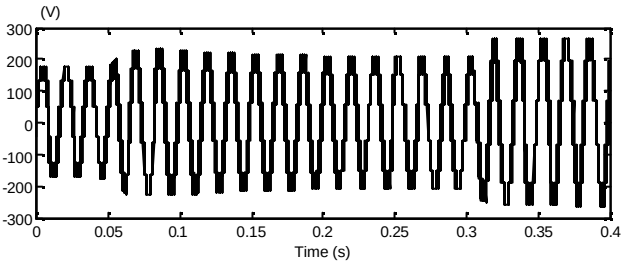


Fig. 11: Phase "*a*" VSC-12pHE output voltage.

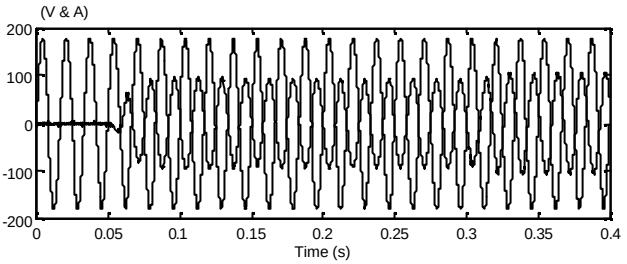


Fig. 12: Phase "*a*" output voltage of the VSC-12pHE and the line current at the PCC.

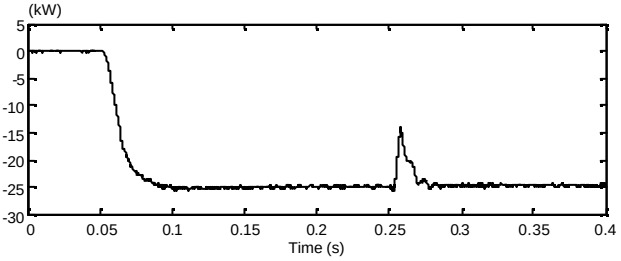


Fig. 13: Instantaneous real power at the VSC-12pHE terminals.

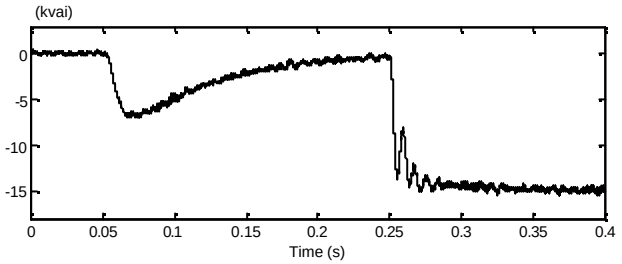


Fig. 14: Instantaneous imaginary power at the VSC-12pHE terminals.

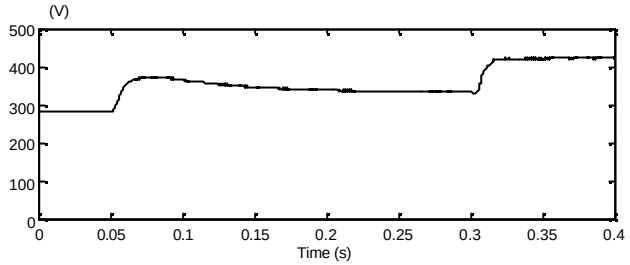


Fig. 15: VSC-12pHE DC link voltage.

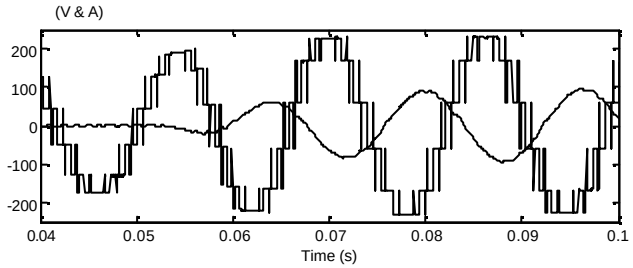


Fig. 16: Detail of VSC-12pHE output voltage and line current

Table I shows the THD of the modeled photovoltaic generation plant in the ATP/EMTP at the PCC considering two basic configurations for the system: (*i*) 12 pulse VSC with programmed harmonic elimination (VSC-12pHE) and (*ii*) 12 pulse VSC with programmed harmonic elimination and LC passive filter (VSC-12pHEf). For simplicity the passive filter was not drawn in Fig. 8 however it is possible to see that the best results are obtained in the second option [5]. The passive filter was designed with a 4000 *rad/s* of cut-off frequency and it was connected at the PCC.

Table I: Measured THD of the system PCC.

| Configuration | THD (%) |
|---|---|
| VSC-12pHE | 8.871 |
| VSC-12pHEf | 2.936 |

## V. CONCLUSIONS

This paper presented some basic concepts and principles of operation of Dispersed Generation System (DGS) based on photovoltaic cells. The use of a combined 12-pulse VSC with programmed harmonic elimination technique improves the output voltage waveform spectrum. The EMTP was used to model and illustrate the operation of the DGS.

Some advantages of 12-pulse converter configuration with harmonic elimination such as: controllability, lower harmonics generation, lower number of VSC were presented and discussed.

## VI. REFERENCES

[1] ELETROBRÁS, Annual Report 1992 (in Portuguese).

[2] R. Ramakumar et al, "Renewable Technologies and Distribution Systems", IEEE Power Engineering Review, Vol. 19, No. 11, Nov. 1999, pp. 5-14.

[3] N.G. Hingorani, "Power Electronics in Electric Utilities: Role of power Electronics in Future power systems", Proc. of the IEEE, Vol. 76, No. 4, April 1988.

[4] N.G. Hingorani, "Introducing Custom Power", IEEE Spectrum, pp. 41-48, June 1995.

[5] ANSI/IEEE Std. 519/1992, "IEEE Guide for Harmonic Control and Reactive Compensation of Static Power Converters", 1992.

[6] S. Mori, K. Matsuno, M. Takeda, M. Seto, "Development of a Large Static Var Generator Using Self-Commutated Inverters for Improving Power System Stability", IEEE Trans. on Power Delivery, Vol. 8, No. 1, February, 1993, pp. 371-377.

[7] C.D. Schauder, E. Stacey, M. Lund, L. Gyugyi, L. Kovalsky, A. Keri, a Meharaban and A. Edris, "AEP UPFC Project: Installation, Commissioning and Operation of The ±160 MVA STATCOM (Phase I)", IEEE Trans. on Power Delivery, Vol.13, No.4, Oct. 1998, pp. 1530-1535.

[8] D.M. Divan, T.A Lipo and T.G. Habetter, "PWM Techniques for Voltage Source Inverters", in *Power Electronics Specialists Conference,* Tutorial Notes, San Antonio, 1990.

[9] N. Mohan et. al, "Power Electronics: Converters, Applications and Design", John Wiley and Sons, 2nd edition, 1994.

[10] Alternative Transients Program Rule Book, Leuven EMTP Center, Belgium, July, 1987.

[11] P.G. Barbosa, A.C.S. de Lima and E.H. Watanabe, "Modelling Thyristors and GTO Based Shunt Compensators for FACTS Applications", Proc. of IV Brazilian Power Electronics Conf. - COBEP, Belo Horizonte, Brazil, Nov./Dec. 1997, pp. 455-460.